

# Structural Analysis of the Binding of Type I, I<sub>1/2</sub>, and II Inhibitors to Eph Tyrosine Kinases

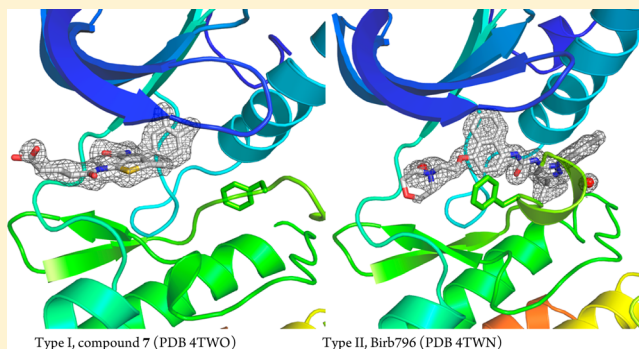
Jing Dong,<sup>\*,†</sup> Hongtao Zhao,<sup>†</sup> Ting Zhou,<sup>†</sup> Dimitrios Spiliotopoulos,<sup>†</sup> Chitra Rajendran,<sup>‡</sup> Xiao-Dan Li,<sup>‡</sup> Danzhi Huang,<sup>†</sup> and Amedeo Caffisch<sup>\*,†</sup>

<sup>†</sup>Department of Biochemistry, University of Zurich, Winterthurerstrasse 190, CH-8057 Zurich, Switzerland

<sup>‡</sup>Laboratory of Biomolecular Research, Paul Scherrer Institut, 5232 Villigen PSI, Switzerland

## S Supporting Information

**ABSTRACT:** We have solved the crystal structures of the EphA3 tyrosine kinase in complex with nine small-molecule inhibitors, which represent five different chemotypes and three main binding modes, i.e., types I and I<sub>1/2</sub> (DFG in) and type II (DFG out). The three structures with type I<sub>1/2</sub> inhibitors show that the higher affinity with respect to type I is due to an additional polar group (hydroxyl or pyrazole ring of indazole) which is fully buried and is involved in the same hydrogen bonds as the (urea or amide) linker of the type II inhibitors. Overall, the type I and type II binding modes belong to the lock-and-key and induced fit mechanism, respectively. In the type II binding, the scaffold in contact with the hinge region influences the position of the Phe765 side chain of the DFG motif and the orientation of the Gly-rich loop. The binding mode of Birb796 in the EphA3 kinase does not involve any hydrogen bond with the hinge region, which is different from the Birb796/p38 MAP kinase complex. Our structural analysis emphasizes the importance of accounting for structural plasticity of the ATP binding site in the design of type II inhibitors of tyrosine kinases.



**KEYWORDS:** Eph kinases, protein crystallography, structure-based drug design, fragment-based docking

The human Eph (erythropoietin-producing hepatocellular) receptors (Ephs) are transmembrane proteins that constitute the largest family of receptor kinases.<sup>1,2</sup> Ephs play a role in embryonic development and in various processes of adult tissues.<sup>3,4</sup> In parallel with their physiological functions, deregulation of Ephs has been implicated in pathologies such as atherosclerosis,<sup>1</sup> diabetes, and Alzheimer's disease.<sup>2</sup> Substantial evidence links deregulation of Ephs to different stages of tumor development (namely, cancer stem cell,<sup>5</sup> angiogenesis, tumor progression, and metastasis<sup>6,7</sup>) mediating both tumor promotion and suppression,<sup>8</sup> consistently with its dichotomous functions in development.<sup>3</sup> It is therefore not surprising that Eph inhibitors are useful to decipher the biology of individual receptors and to act as prognostic and/or diagnostic tools.<sup>9</sup> In this framework, many efforts have been devoted to the quest for specific inhibitors of individual Eph kinase domains with potential antiangiogenic and/or antitumor activity.<sup>10–14</sup>

Here, we present a comparative analysis of crystal structures of the EphA3 tyrosine kinase in complex with small molecule inhibitors (Table 1). Except for the Birb796 inhibitor, which was discovered by others,<sup>15</sup> all inhibitor chemotypes were identified in silico by fragment-based high-throughput docking.<sup>16,17</sup> The docked poses were ranked according to a force-field based energy function with continuum electrostatic solvation or by semiempirical quantum mechanical calcula-

tions.<sup>18</sup> Optimization was carried out by synthesis of a small set of derivatives ranging from only one<sup>12</sup> to about 25 compounds.<sup>13,14</sup>

The orientation of the Phe765 side chain of the DFG motif (the Asp-Phe-Gly tripeptide segment at the beginning of the activation loop) is used to classify the binding modes. In the binding modes of types I and I<sub>1/2</sub>, the Phe765 side chain points inside (DFG in) toward the so-called hydrophobic spine, while it points outside (DFG out) in the type II inhibitors whose additional hydrophobic moiety occupies the allosteric pocket originating from the displacement of the DFG Phe.<sup>19–21</sup> The Protein Databank (PDB) contains only four crystal structures of Eph tyrosine kinases in complex with inhibitors of type II (PDB codes 4P5Z, 4TWN, 3DZQ,<sup>22</sup> and 3DKO<sup>22</sup>). Concerning type I<sub>1/2</sub> inhibitors, there are three complexes with EphA3 (4GK2, 4GK4, and 4G2F), and two with EphB4 (2X9F<sup>23</sup> and 2XVD<sup>24</sup>). The type I inhibitors are the most abundant (nearly 50 structures).

**Special Issue:** New Frontiers in Kinases

**Received:** September 1, 2014

**Accepted:** September 29, 2014

**Published:** September 29, 2014

Table 1. Crystal Structures of EphA3 Inhibitors

	Compound <sup>a</sup>	Binding mode	PDB code	IC <sub>50</sub> <sup>b</sup> (nM)	Ref.
1		I	4GK3	56	13
2		I <sub>1/2</sub>	4GK2	5	10, 13
3		I <sub>1/2</sub>	4GK4	14	13
4		I	4P4C	300	14
5		I	4P5Q	3000	14
6		II	4P5Z	N.A.	14
7		I	4TWO	8000	18 <sup>c</sup>
8		I <sub>1/2</sub>	4G2F	300	12
Birb796		II	4TWN	N.A.	This work
AWL-II-38.3		II	3DZQ	N.A.	22

<sup>a</sup>The crystal structures are grouped by binding mode in Figures 1 and 2 and by chemotype in Figures S2–S5 of the Supporting Information. <sup>b</sup>FRET-based enzymatic assay for EphB4 with ATP concentration of 30  $\mu$ M. Note that the ATP binding site residues are identical in EphA3 and EphB4. <sup>c</sup>The crystal structure was not published in the original paper on the in silico discovery of this compound. The electron density is shown in Figure S1, Supporting Information.

Our four crystal structures with type I inhibitors correspond to three different chemotypes: xanthine (compound 1 in Table 1, PDB code 4GK3<sup>10,13</sup>), quinoxalines (4 and 5, PDB codes 4P4C and 4P5Q, respectively<sup>14</sup>), and thiophene-3-carboxamide (7, 4TWO,<sup>18</sup> Figure S1 in the Supporting Information). The

three type I<sub>1/2</sub> inhibitors belong to two chemotypes: xanthine (2 and 3, PDB codes 4GK2 and 4GK3, respectively<sup>10,13</sup>) and another fused 3-ring system (8, 4G2F<sup>12</sup>). Compared to the type I inhibitors, the type I<sub>1/2</sub> inhibitors have an additional polar group (hydroxyl or indazole, Table 1), which is involved in buried, and thus very favorable, hydrogen bonds with the Glu670 side chain of the C helix and the backbone NH of the DFG Asp (Figure 1). The Phe765 of the DFG motif occupies the hydrophobic pocket also in the type I<sub>1/2</sub> inhibitors. Moreover, the binding mode and overall structure of EphA3

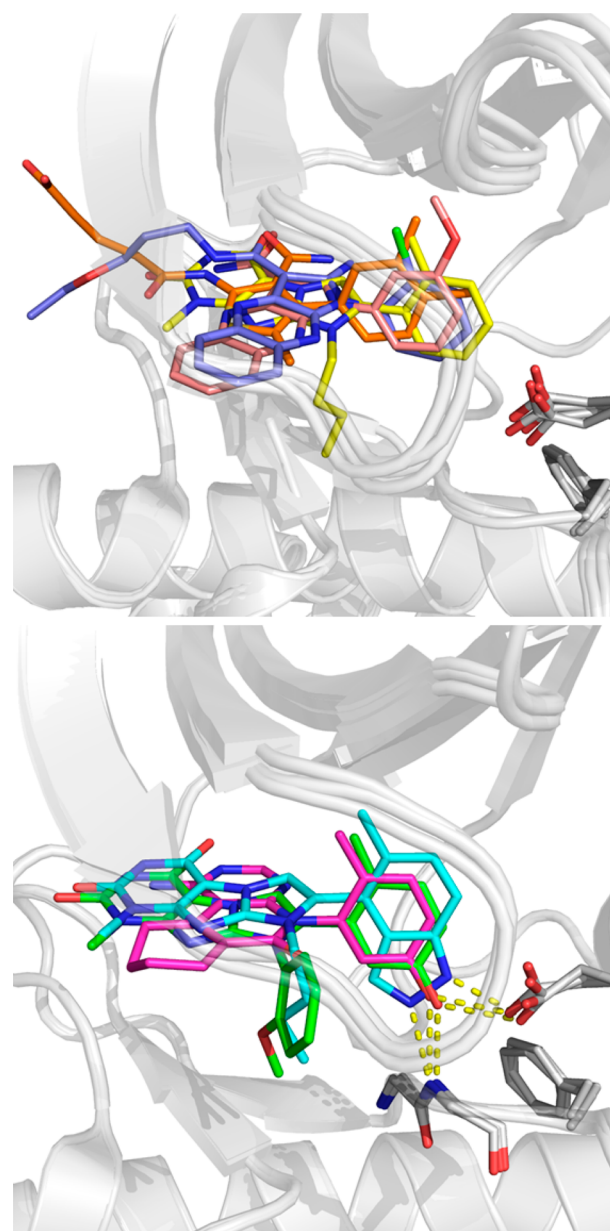


**Figure 1.** Crystal structures of EphA3 in complex with inhibitors that preserve the DFG-in conformation. (Top) Type I inhibitors 1 (carbon atoms in yellow, PDB code 4GK3), 4 (salmon, 4P4C), 5 (blue, 4P5Q), and 7 (orange, 4TWO). (Bottom) Type I<sub>1/2</sub> inhibitors 2 (green, 4GK2), 3 (cyan, 4GK4), and 8 (magenta, 4G2F). The side chains of the DFG motif Phe765 and the Glu670 of the C helix are also shown (carbon atoms in gray). All nitrogen and oxygen atoms are in blue and red, respectively. The C $\alpha$  atoms of EphA3 were used for the structural superposition in all figures.

are essentially identical for the four inhibitors of type I and the three type  $I_{1/2}$  inhibitors (Figure 1). Quantitatively, the pairwise root-mean-square deviation of the  $C_\alpha$  atoms is smaller than 0.3 Å for the seven EphA3 structures with inhibitors of type I and  $I_{1/2}$  listed in Table 1, and considering all of the 50 EphA/B structures with type I and  $I_{1/2}$  inhibitors in the PDB, it is almost always smaller than 1.0 Å. Thus, type I and  $I_{1/2}$  inhibitors binding to Eph tyrosine kinases reflects the lock-and-key model.

In sharp contrast to the structures with type I and  $I_{1/2}$  inhibitors, there is significant variability of the ATP binding site for the type II binding mode (Figure 2). The activation loop

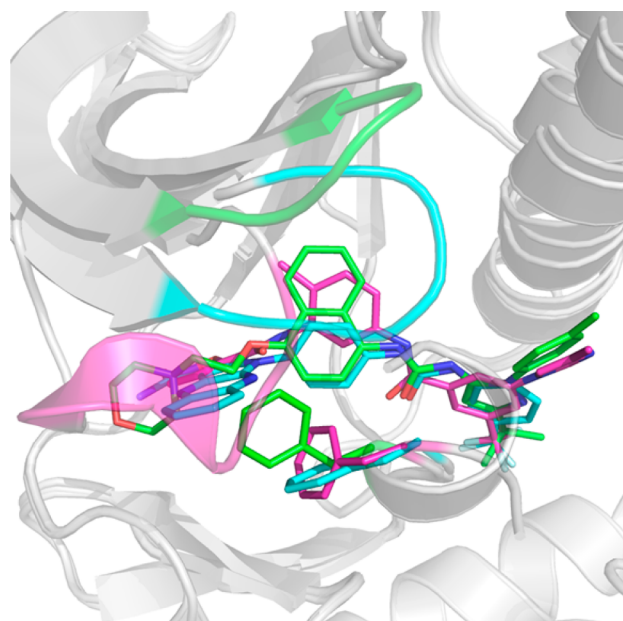


**Figure 2.** Crystal structures of EphA3 in complex with type II inhibitors **6** (carbon atoms in cyan, 4PSZ), Birb796 (green, 4TWN), and AWL-II-38.3 (magenta, 3DZQ). The tip of the Gly-rich loop is colored according to the inhibitor.

assumes a close conformation and the DFG-motif partially occupies the ATP binding site. Interestingly, the Phe765 side chain of the DFG-motif is positioned according to the scaffold of the type II inhibitors. The conjugated 3-ring scaffold of the type II inhibitor **6** (4PSZ) is involved in a  $\pi$ -stacking interaction with the Phe765 side chain of the DFG-motif (cyan structure in Figures 2 and S4, Supporting Information). However, for type II inhibitors with small hinge-binding moiety, e.g., the isoxazole ring of the inhibitor AWL-II-38.3 (3DZQ), the phenyl ring of the DFG-motif moves further inward to tightly encompass the hinge-binding moiety. Furthermore, the glycine-rich loop is collapsed into the ATP binding site to completely seal the hinge-binding moiety in the ATP-site (magenta structure in Figure 2). Thus, the volume of the ATP-binding site in 3DZQ is significantly reduced with respect to the other complexes of EphA3 with type II inhibitors (*viz.* compound **6** and Birb796, PDB codes 4PSZ and 4TWN, respectively). The same is observed for the complex of EphA7 and the nicotinamide-based inhibitor (3DKO). The structural variability indicates that type II inhibitors bind by the induced fit mechanism.

It is important to consider the practical consequences of the structural plasticity of the ATP binding site. In particular, cross docking of type II inhibitors would be much less successful than type I inhibitors. As an example, cross docking of inhibitors **6**

and Birb796 into 3DZQ is impossible because of steric conflicts. These observations are consistent with the paucity of type II inhibitors and the tiny fraction of explored chemical space,<sup>25</sup> which is in strong contrast with the large number of type I inhibitors, many of which have been identified by virtual screening. The small chemical space explored by type II compounds is reflected in the use of two main linkers (*viz.* amide and urea) and a small set of hydrophobic groups in the allosteric pocket (e.g., trifluoromethylphenyl).

Previously, we reported a novel class of type II inhibitors based on a conformation generated by molecular dynamics simulations with the aim to increase the aperture of the binding site.<sup>26</sup> Unlike the DFG-in conformation, it relies on a type II inhibitor to stabilize the protein into a scarcely populated DFG-out conformation. Given the induced fit mechanism of type II inhibitors, experimental exploration of the DFG-out configuration space is likely to be difficult. In light of this difficulty and our own experience with *in silico* screening of type II inhibitors, molecular dynamics, combined with subsequent ensemble docking, may open new horizons in the design of type II kinase inhibitors by exploring conformational space inaccessible to experiments.<sup>16</sup>

The structural overlap of the complex of Birb796 with EphA3 (PDB code 4TWN) and p38 MAP kinase (1KV2) reveals a similar type II binding (green and salmon in Figure 3). Upon

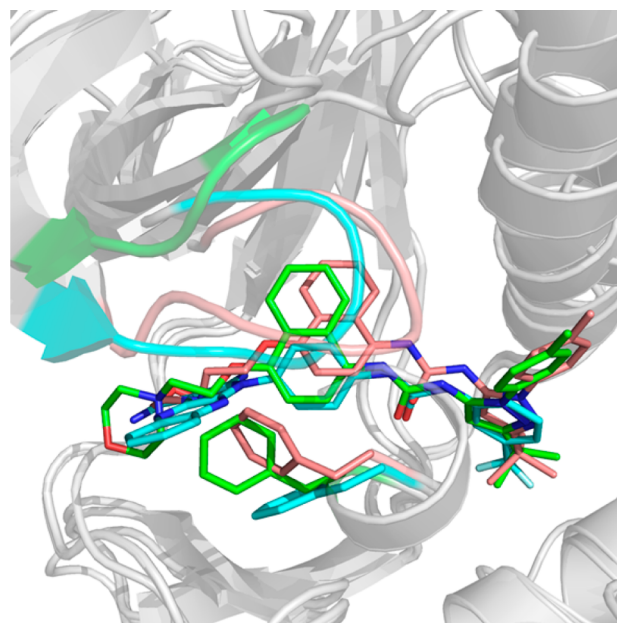


**Figure 3.** Crystal structures of EphA3 in complex with type II inhibitors **6** (carbon atoms in cyan, 4PSZ) and Birb796 (green, 4TWN), and the complex of the p38 Map kinase with Birb796 (salmon, 1KV2). The tip of the Gly-rich loop is colored according to the inhibitor.

structural overlap of the catalytic domain of the two kinases, the deviation of most atoms of Birb796 is below 1.0 Å, but there are significant differences in the orientation of the morpholino ring. Interestingly, the only hydrogen bond of Birb796 with the hinge region of p38 MAP (between the oxygen atom of the morpholino and the NH of Met109 in the hinge region) is not present in the complex with EphA3 as the morpholino ring is more exposed toward the solvent and a water molecule acts as hydrogen bond acceptor for the NH of Met702 in the EphA3



hinge region (Figure 4). Furthermore, the differences in the orientation of the aromatic ring of the Phe765 side chain of the

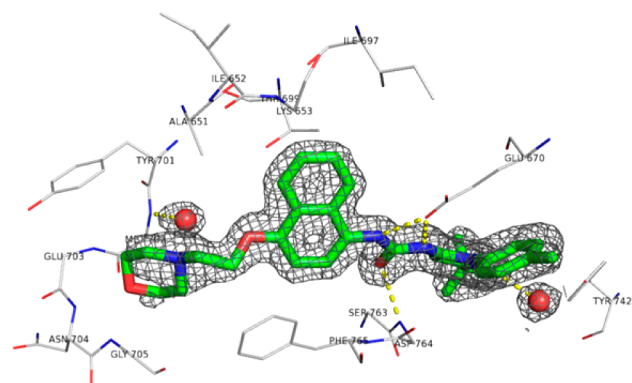


**Figure 4.** Crystal structures of EphA3 (carbon atoms in gray) in complex with Birb796 (green, PDB code 4TWN). The  $2mF_o - DF_c$  electron density map contoured at  $1\sigma$  (gray mesh) was generated in a region within 1.6 Å for Birb796 and two water molecules (red spheres).

DFG motif are probably a consequence of the different positions of the morpholino ring (green and salmon in Figure 3). There are other structures of Birb796 in complex with protein kinases, e.g., B-raf (4JVJ), JNK2 (3NPC), and PYK2 (3FZS). These structures show also variable positions and orientations of the morpholino group of Birb796 and the Phe residue of the DFG motif.

The Gly-rich loop, and particularly its tip, is much closer to the ATP binding site in the complex of Birb796 with p38 MAP kinase than with EphA3 (salmon and green in Figure 3). Remarkably, the same loop in the Birb796/p38 complex assumes an orientation almost identical as the one in the complex of the quinoxaline **6** with EphA3 (salmon and cyan in Figure 3). Considering that in these three structures the Gly-rich loop is not involved in crystal contacts, these observations are rather surprising as they indicate that the Gly-rich loop orientations in two kinases (p38 MAP and EphA3) with the same inhibitor (Birb796) are more different than for two different inhibitors (p38/Birb796 and EphA3/compound **6**).

In conclusion, we have presented a comparative analysis of the binding mode of a dozen inhibitors of the EphA3 tyrosine kinases, eight of which represent four different scaffolds (from monocyclic to fused 3-ring systems, Table 1), which were identified by fragment-based docking. The conformation of the ATP binding site is remarkably similar in the structures with inhibitors of types I and I<sub>1/2</sub>. In contrast, for the type II binding mode (DFG out) the chemotype interacting with the hinge region determines the conformation of the flexible Gly-rich loop, as well as the position and orientation of the Phe765 side chain of the DFG motif. Thus, the identification of type II binders in silico, by cross-docking into an apo structure or structure with type I inhibitor, is difficult because of the induced fit mechanism of type II binding.

## ■ ASSOCIATED CONTENT

### Supporting Information

Experimental methods, X-ray crystal structure statistic data, and structural analyses of all reported crystal structures. This material is available free of charge via the Internet at <http://pubs.acs.org>.

## Accession Codes

The PDB codes for the kinase domain of EphA3 in complex with the inhibitors **7** and Birb796 are 4TWO and 4TWN, respectively.

## ■ AUTHOR INFORMATION

### Corresponding Authors

\*(J.D.) E-mail: [j.dong@bioc.uzh.ch](mailto:j.dong@bioc.uzh.ch).

\*(A.C.) E-mail: [caflisch@bioc.uzh.ch](mailto:caflisch@bioc.uzh.ch). Phone: (41) 446355521.

### Author Contributions

All authors contributed to this work. The crystal structures were solved by J.D. The manuscript was written mainly by H.Z. and A.C.

### Funding

This work was supported by grants of the Swiss National Science Foundation and the Swiss Cancer League (Krebsliga). D.S. is a recipient of the SystemsX.ch translational postdoc fellowship.

### Notes

The authors declare no competing financial interest.

## ■ ACKNOWLEDGMENTS

We thank Prof. Sirano Dhe-Paganon for providing the plasmid used for EphA3 expression. We thank Dr. Karine Lafleur, Dr. Andrea Unzue, and Prof. Cristina Nevado for the synthesis of compounds **1–3**, **6**, and **8**.

## ■ REFERENCES

- (1) Tognolini, M.; Hassan-Mohamed, I.; Giorgio, C.; Zanotti, I.; Lodola, A. Therapeutic perspectives of Eph-ephrin system modulation. *Drug Discovery Today* **2014**, *19*, 661–9.
- (2) Pasquale, E. B. Eph-ephrin bidirectional signaling in physiology and disease. *Cell* **2008**, *133*, 38–52.
- (3) Boyd, A. W.; Bartlett, P. F.; Lackmann, M. Therapeutic targeting of Eph receptors and their ligands. *Nat. Rev. Drug Discovery* **2014**, *13*, 39–62.
- (4) Wang, Y. D.; Nakayama, M.; Pitulescu, M. E.; Schmidt, T. S.; Bochenek, M. L.; Sakakibara, A.; Adams, S.; Davy, A.; Deutsch, U.; Luthi, U.; Barberis, A.; Benjamin, L. E.; Makinen, T.; Nobes, C. D.; Adams, R. H. Ephrin-B2 controls VEGF-induced angiogenesis and lymphangiogenesis. *Nature* **2010**, *465*, 483–U108.
- (5) Chen, J.; Song, W.; Amato, K. Eph receptor tyrosine kinases in cancer stem cells. *Cytokine Growth Factor Rev.* **2014**, DOI: 10.1016/j.cytogfr.2014.05.001.
- (6) Hatziaepostolou, M.; Polytrachou, C. Eph/ephrin system: In the quest of novel anti-angiogenic therapies. *Br. J. Pharmacol.* **2014**, DOI: 10.1111/bph.12718.
- (7) Kuijper, S.; Turner, C. J.; Adams, R. H. Regulation of angiogenesis by Eph-ephrin interactions. *Trends Cardiovasc. Med.* **2007**, *17*, 145–51.
- (8) Chen, J.; Zhuang, G.; Frieden, L.; Debinski, W. Eph receptors and Ephrins in cancer: common themes and controversies. *Cancer Res.* **2008**, *68*, 10031–3.
- (9) Gucciardo, E.; Sugiyama, N.; Lehti, K. Eph- and ephrin-dependent mechanisms in tumor and stem cell dynamics. *Cell. Mol. Life Sci.* **2014**, *71*, 3685–3710.
- (10) Lafleur, K.; Huang, D.; Zhou, T.; Caflisch, A.; Nevado, C. Structure-based optimization of potent and selective inhibitors of the tyrosine kinase erythropoietin producing human hepatocellular carcinoma receptor B4 (EphB4). *J. Med. Chem.* **2009**, *52*, 6433–46.
- (11) Martiny-Baron, G.; Holzer, P.; Billy, E.; Schnell, C.; Brueggen, J.; Ferretti, M.; Schmiedebeg, N.; Wood, J. M.; Furet, P.; Imbach, P. The small molecule specific EphB4 kinase inhibitor NVP-BHG712 inhibits VEGF driven angiogenesis. *Angiogenesis* **2010**, *13*, 259–67.

(12) Zhao, H. T.; Dong, J.; Lafleur, K.; Nevado, C.; Caflich, A. Discovery of a novel chemotype of tyrosine kinase inhibitors by fragment-based docking and molecular dynamics. *ACS Med. Chem. Lett.* **2012**, *3*, 834–838.

(13) Lafleur, K.; Dong, J.; Huang, D.; Caflich, A.; Nevado, C. Optimization of inhibitors of the tyrosine kinase EphB4. 2. Cellular potency improvement and binding mode validation by X-ray crystallography. *J. Med. Chem.* **2013**, *56*, 84–96.

(14) Unzue, A.; Dong, J.; Lafleur, K.; Zhao, H.; Frugier, E.; Caflich, A.; Nevado, C. Pyrrolo[3,2-b]quinoxaline derivatives as types I and II Eph tyrosine kinase inhibitors: Structure-based design, synthesis, and in vivo validation. *J. Med. Chem.* **2014**, *57*, 6834–6844.

(15) Pargellis, C.; Tong, L.; Churchill, L.; Cirillo, P. F.; Gilmore, T.; Graham, A. G.; Gröb, P. M.; Hickey, E. R.; Moss, N.; Pav, S.; Regan, J. Inhibition of p38 MAP kinase by utilizing a novel allosteric binding site. *Nat. Struct. Biol.* **2002**, *9*, 268–72.

(16) Zhao, H.; Caflich, A. Molecular dynamics in drug design. *Eur. J. Med. Chem.* **2014**, DOI: 10.1016/j.ejmech.2014.08.004.

(17) Huang, D.; Caflich, A. Library screening by fragment-based docking. *J. Mol. Recognit.* **2010**, *23*, 183–93.

(18) Zhou, T.; Caflich, A. High-throughput virtual screening using quantum mechanical probes: discovery of selective kinase inhibitors. *ChemMedChem* **2010**, *5*, 1007–14.

(19) Liu, Y.; Gray, N. S. Rational design of inhibitors that bind to inactive kinase conformations. *Nat. Chem. Biol.* **2006**, *2*, 358–64.

(20) Zuccotto, F.; Ardini, E.; Casale, E.; Angiolini, M. Through the "gatekeeper door": exploiting the active kinase conformation. *J. Med. Chem.* **2010**, *53*, 2681–94.

(21) Traxler, P.; Furet, P. Strategies toward the design of novel and selective protein tyrosine kinase inhibitors. *Pharmacol. Ther.* **1999**, *82*, 195–206.

(22) Choi, Y.; Syeda, F.; Walker, J. R.; Finerty, P. J., Jr.; Cuerrier, D.; Wojciechowski, A.; Liu, Q.; Dhe-Paganon, S.; Gray, N. S. Discovery and structural analysis of Eph receptor tyrosine kinase inhibitors. *Bioorg. Med. Chem. Lett.* **2009**, *19*, 4467–70.

(23) Bardelle, C.; Barlaam, B.; Brooks, N.; Coleman, T.; Cross, D.; Ducray, R.; Green, I.; Brempt, C. L.; Olivier, A.; Read, J. Inhibitors of the tyrosine kinase EphB4. Part 3: identification of non-benzodioxole-based kinase inhibitors. *Bioorg. Med. Chem. Lett.* **2010**, *20*, 6242–5.

(24) Barlaam, B.; Ducray, R.; Lambert-van der Brempt, C.; Ple, P.; Bardelle, C.; Brooks, N.; Coleman, T.; Cross, D.; Kettle, J. G.; Read, J. Inhibitors of the tyrosine kinase EphB4. Part 4: Discovery and optimization of a benzylic alcohol series. *Bioorg. Med. Chem. Lett.* **2011**, *21*, 2207–11.

(25) Zhao, H.; Caflich, A. Current kinase inhibitors cover a tiny fraction of fragment space. Submitted.

(26) Zhao, H.; Huang, D.; Caflich, A. Discovery of tyrosine kinase inhibitors by docking into an inactive kinase conformation generated by molecular dynamics. *ChemMedChem* **2012**, *7*, 1983–90.